Rock and Soil Mechanics

Volume 41 | Issue 1 Article 11

9-23-2020

Preliminary study on real-time pore water pressure response and reinforcement mechanism of air-booster vacuum preloading treated dredged slurry

Li SHI
Department of Architecture Engineering, Zhejiang University of Technology, Hangzhou, Zhejiang 310014, China;

Dong-dong HU
Department of Architecture Engineering, Zhejiang University of Technology, Hangzhou, Zhejiang 310014, China;

Yuan-qiang CAI
Department of Architecture Engineering, Zhejiang University of Technology, Hangzhou, Zhejiang 310014, China;

Xiao-dong PAN
Department of Architecture Engineering, Zhejiang University of Technology, Hangzhou, Zhejiang 310014, China;

See next page for additional authors

Custom Citation

SHI Li, HU Dong-dong, CAI Yuan-qiang, PAN Xiao-dong, SUN Hong-lei, . Preliminary study on real-time pore water pressure response and reinforcement mechanism of air-booster vacuum preloading treated dredged slurry[J]. Rock and Soil Mechanics, 2020, 41(1): 185-193.

Preliminary study on real-time pore water pressure response and reinforcement mechanism of air-booster vacuum preloading treated dredged slurry

Authors

Li SHI, Dong-dong HU, Yuan-qiang CAI, Xiao-dong PAN, and Hong-lei SUN

Rock and Soil Mechanics 2020 41(1): 185−193 ISSN 1000−7598
https: //doi.org/10.16285/j.rsm.2018.7192 rocksoilmech.researchcommons.org/journal

Preliminary study on real-time pore water pressure response and reinforcement mechanism of air-booster vacuum preloading treated dredged slurry

SHI Li[1], HU Dong-dong[1], CAI Yuan-qiang[1], PAN Xiao-dong[1], SUN Hong-lei[2]

1. Department of Architecture Engineering, Zhejiang University of Technology, Hangzhou, Zhejiang 310014, China;
2. Department of Architecture Engineering, Zhejiang University, Hangzhou, Zhejiang 310058, China

Abstract: Laboratory tests have been carried out for simulating dredged-slurry treatment combining air-booster and conventional vacuum preloading methods. Settlement plate, micro pore water pressure transducer and miniature vane shearing instrument are adopted for monitoring the settlement, the pore pressure dissipation and the soil strength during the test. The tests results demonstrate that the air-booster vacuum-preloading method can significantly improve the soil strength, pore-water pressure dissipation and settlement. In particular, the real-time responses of pore-water pressure during the air-pressurizing process have been obtained that, in combination with the numerical simulations, help derive the reinforcement mechanism of the air-booster vacuum preloading method, which involves using micro cracks generated by splitting soil between the booster tube and PVD using the pressurised air. Those cracks improve the soil permeability, and have lasting effect even after air pressuring ceased.

Keywords: air pressurizing; vacuum preloading; reinforcement effect; reinforcement mechanism

1 Introduction

Large volumes of dredged slurry will be produced due to the land reclamation in coastal areas and the river channel dredging inland. The dredged slurry is of very high water content, large void ratio and high compressibility, and thus of little bearing capacity. It has to be improved before using for engineering construction, such as factories, roads and buildings [1].

The vacuum preloading method is commonly used for improving the dredged slurry. Considerable research efforts have been conducted to investigate various factors associated with vacuum preloading method, including vacuum degree, settlement, pore water pressure, consolidation degree, reinforcement depth and implementation method [2-8].

Existing experimental studies and engineering practices have reported that during vacuum preloading only the slurries in shallow depth and near the vertical drains can be effectively improved, i.e. while the improvement for deeper slurries is very limited[9-10], even if the vacuum preloading time is elongated. Most researchers attribute this phenomenon to the high water content (80%−120%) of dredged slurry, as the stable soil skeleton is not formed yet under self-weight consolidation, which results in migration of slurry particles under the vacuum gradient and then the formation of dense soil layers on the surfaces of prefabricated vertical drain (PVD). For the dragging forces exerted on the slurry particles with mean diameters of 5−10 μm (typical size) by the vacuum (e.g. 80 kPa, a typical vacuum level in practice) are 10-20 times of their gravitation forces [12]. As a result, the void ratio of the dense soil layer is much lower than that of the natural soft soil (i.e. particles compacted under self-weight), which makes the vacuum pressure attenuates in the radial direction. Therefore, improvement on dredged slurries by conventional vacuum preloading method is not good.

To overcome the deficiency, research have been conducted to improve the conventional vacuum preloading method. For example, a hand-shaped connector was designed to connect the vacuum tube and the head of the PVD to improve the vacuum degree in PVD [1];lime or the polyacrylamide were added to the dredged slurry to flocculate the slurry particles [13]; electric field was used in combination with the vacuum field to enhance the seepage consolidation of the soft soil [14]; a pervious tube or PVD was inserted to booster air into the soil to improve the consolidation of the slurry (the so called air-booster vacuum preloading technology in literature [15]).

It has been demonstrated both in field test [16] and laboratory study [17] that pressurizing the soil by air can help improving the treatment effects of the vacuum preloading method. However, no agreement has been reached on the mechanism of the observed promotion in seepage consolidation of the dredged slurry due to the boosted air in soil. Cai et al. [15] analyzed the mechanism from the incremental stress analysis for a soil element between the booster tube and the PVD. Yan et al. [18] found that the booster air increases the pressure difference between the booster tube and the PVD, and thus enhances the seepage of the pore water. Zhang et al. [19] indicated that the pressurized air would generate cracks within the soft soil, and the cracks help increase seepage paths and thus accelerate the drainage consolidation process. Those cracks would remain open after the air boosting stopped.

Laboratory test on the dredged slurry treated by the air-booster vacuum preloading method has been conducted in this study to evaluate the effects of air pressurizing on the drainage consolidation of the slurry. The improvements on the

Received: 3 December. 2018 Revised: 14 May 2019
This work was supported by the National Key R&D Program of China (2016YFC0800200), the National Natural Science Foundation of China (51620105008, 51608482, 51879234) and the Key R&D Program of Zhejiang Province (2018C03038).
First author: SHI Li, male, born in 1987, PhD, associate Professor, Research interest: geotechnical engineering. E-mail: lishi@zjut.edu.cn

settlement, the pore water pressure dissipation and the shear strength of the soil have been quantitatively analyzed by comparing with the results from conventional vacuum preloading test (i.e. model test without air pressurizing). The real-time response of the pore water pressure were recorded during the course of air pressurization. Based on the test results and the finite element modeling results, the mechanism of promotions in drainage consolidation of the dredged slurry by the air pressurizing has been analyzed and discussed.

2 Model test

2.1 Soil sample

The test soil was sampled from a tideland reclamation site located at Dongtou area of Wenzhou, Zhejiang, China. The basic physical and mechanical properties of the soil sample are summarized in Table 1. The particle gradation curve of the soil sample is given in Fig.1.

Table 1 Physical and mechanical properties of dredged slurry

Density /(g • cm^{-3})	Water content /%	Specific gravity	Liquid limit /%	Plastic limit /%	Average diameter
1.52	95.00	2.68	53	32	5

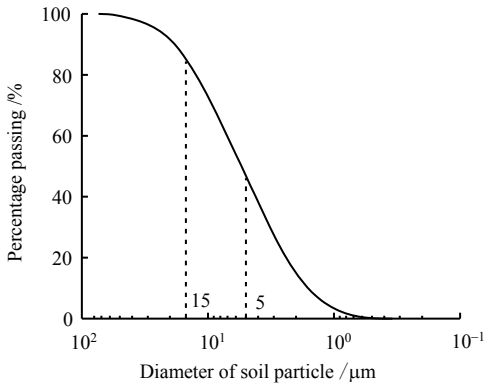

Fig.1 Particle size distribution curve of soil sample

2.2 Test apparatus

A self-developed apparatus consisting of a steel bucket, a vacuum pump, an air/moisture separator, an air booster pump, a pressure regulating valve, a data acquisition system and a sealing system, was adopted for the laboratory test on vacuum consolidation of dredged slurry. The vacuum pressure and the pressurized air were applied through tubes connected to the box through a specifically-designed opening at side wall of the box, which could solve the air leakage problem associating with tube connections through the openings of the sealing membrane on top of the box. The steel bucket had a diameter of 0.5 m and height of 0.6 m. The sealing system included membrane, geotextile, hand-shaped connector, and rubber plugs, etc. The data acquisition system had displacement transducer (LVDT), vacuum gauge, pressure gauge, electronic balance, and micro pore-water-pressure (PWP) sensors. The micro PWP sensor had small size (6 mm in diameter), large measurement range (-100−100 kPa) and high accuracy (0.4 kPa in sensitivity). The telescopic LVDT transducer had a measurement range of 0−20 cm and a sensitivity of 1 mm. The data sampling frequency was set to 1 Hz during the test.

2.3 Test procedures

Two parallel tests were conducted as shown in Fig. 2. One was for the conventional vacuum consolidation of the dredged slurry (Test A). The other is the air-booster vacuum consolidation of the dredged slurry (Test B). The operating procedures of the two tests were briefed as: Step 1, one PVD and three PWP transducers were fixed to a racket made of thin steel wire. The horizontal distances between the transducers and the PVD were 0 cm (i.e. right against the PVD membrane), 10 cm, and 20 cm, respectively. And the three transducers were placed at the same height, i.e. 20 cm above the racket bottom. The same rackets were placed into the buckets of the two tests; Step 2, the vacuum tube and the wires connected to the transducers exited the bucket through the side opening; Step 3, the evenly mixed slurry (See Table 1) was poured into the bucket to the height of 0.55 m; Step 4, one layer of geotextile and two layers of airtight membranes were placed on top of the slurry; Step 5, a lid was placed and fastened to top of the bucket using bolts. The edge of the geotextile and membrane between the lid bottom and the bucket top were clamped to make the system airtight. The same LVDT transducers were placed on top of the membrane at the same locations for the two tests; Step 6, the vacuum pump was turn on, and the vacuum preloading lasted for 35 consecutive days; Step 7, after the test accomplished, in-situ micro vane tests were conducted for both tested soils to measure the shear strength.

The special procedures for Test B were: in Step 1, a booster tube (made of spiral steel-wire skeleton covered by permeable filter cloth) was fixed to the further side of the racket; in Step 2, the tube connecting to the booster tube exited the bucket through the side opening; in Step 6, two air boosting tests were carried out at the middle and the late stages of the vacuum preloading period, respectively. For the middle-stage air boosting, the air boost pump worked on the 19th, 20th and 21st day of the vacuum treatment period (i.e. 35 days). For the late-stage one, the boost pump worked on the 32nd and 33rd day.

In engineering implementation of the air pressurization, parameters including both the buried depth and the length of the booster tube, the boosting pressure, the boosting duration, and the time to start boosting have important effects on the air-booster vacuum preloading method. The head of the booster tube is typically buried 2 m below the ground. The length of the booster tube for air flow is typically 5-8 m, which is 20%-40% of the installation depth of PVD. However, the values of the boosting pressure are quite different based on current studies[20-22]. In practice, the booster pump works in an intermittent manner, e.g., the boosting time is 2-8 hours per day. Moreover, the boosting typically starts at the middle and late stages of the vacuum preloading period. It should be noted that the vacuum pump continues to work during the air boosting period. It is concluded from above that the parameters associated with air boosting are largely determined by engineering experiences. No quantitative guidelines have been

established by the industry or the academy societies. For the model test in this paper, the length of the booster tube is 12 cm which is about 34% of the PVD length (35 cm). However, due to the limited size of the bucket (the soil height is 0.55 m), a small value (20 kPa) is set to the boosting pressure, so the possible destroy of the whole sealing system can be avoided. The boosting time is chosen as 10 mins per day to avoid too much air accumulated in soil and the resultant destroys of the soil and the sealing system. A similar boosting time has been reported in the literature [20].

2.4 Boundary conditions and drainage paths

As shown in Fig.2, the side walls and the bottom of the steel bucket can be deemed as fixed and impervious boundaries, which correspond to the no-displacement and no-flux boundary conditions at the edge of the influence zone that are commonly adopted in drain-well consolidation theory for the PVD treated soft ground (the PVDs are inserted generally in a triangular or rectangular pattern). There is no drainage on top of the slurry because of the airtight membrane; however, the slurry is free to settle. Those boundary conditions are the same as those the vacuum preloading in engineering practice. As for the drainage paths of the model test, the pore water of the slurry seeps into the PVD first, and then it flows into the separator through the tubes.

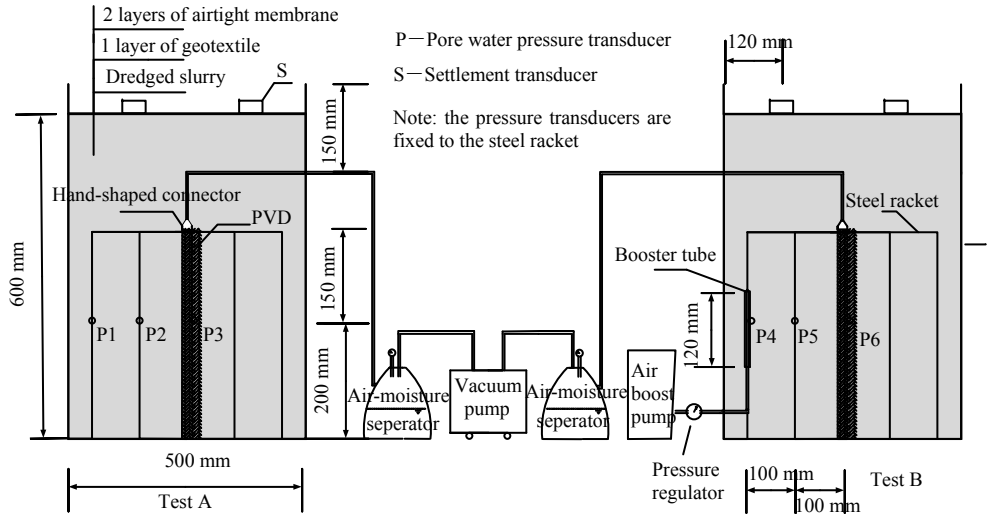

Fig.2 Schematic diagram of test models

3 Test results

3.1 Settlement

Fig.3 compares the settlement variation with respect to time for both Test A and B. It is seen from the figure that the settlement rate of Test B is slightly higher than that of Test A within the first 5 days. The difference is attributed to the inevitable minor discrepancy in wire and tube connection and arrangement between Test A and B. However, it is observed that the settlement rate of Test B gradually decreases to approach that of Test A during the period from the 6 th day to the day before the middle-stage air boosting. For the air boosting at the middle stage (i.e. from the 19th day to 21st day), obvious increase in the settlement rate can be observed for Test B, i.e. the settlement rate is 7 mm/d as compared to the value of 4 mm/d for the average of three days before the boosting. It is noted that in Test A the settlement rate is 3 mm/d for the same time period. For the time gap between the boosting at the middle and the late stages, it is seen from Fig.3 that the settlement rate of Test B decreases to 3.5 mm/d, which is still larger than the corresponding value of 2.6 mm/d for Test A. For the air boosting at the late stage (i.e. from 32nd to 33rd day), another increased settlement rate (5 mm/d) for Test B can be observed. When both test were stopped on the 35th day, the final settlement of Test B is 18.2 cm as compared to 15.1 cm of Test A. In other words, the air-booster vacuum preloading method (Test B) can achieve settlement 20.5% higher than that induced by conventional vacuum preloading method (Test A).

3.2 Pore water pressure

Figs.4(a) and (b) present the dissipations of excess pore water pressure (PWP) recorded at the three transducers for Test A and B, respectively, for the entire treatment period. The PWP at 12 o'clock of each day is extracted and presented in this figure.

It is seen that the PWP dissipation increases obviously during the period of middle-stage air boosting as well as the time period shortly after the boosting. Take PWP transducer P6 as an example, its dissipation rate increases from 1.05 kPa/d to 6.09 kPa/d for the time periods before and after the first boosting, respectively. For comparison, the corresponding PWP dissipation rate at PWP transducer P3 from Test A is 2.3 kPa/d during the first boosting period. For the second boosting (i.e. the late-stage air boosting), similarly, an increased dissipation rate can be observed for Test B. The accumulated PWP dissipations of Test A and B are 74.41 kPa and 78.62 kPa (the value is the average of the three transducers), respectively, when both test were stopped on the 35th day. Thus, the air-booster vacuum preloading technology can promote the PWP dissipation.

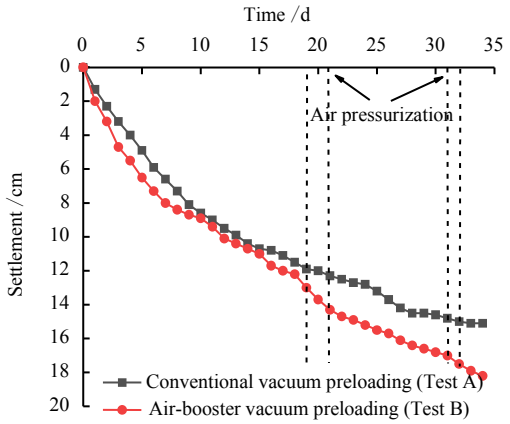

Fig.3 Variations of surface settlement with respect to time

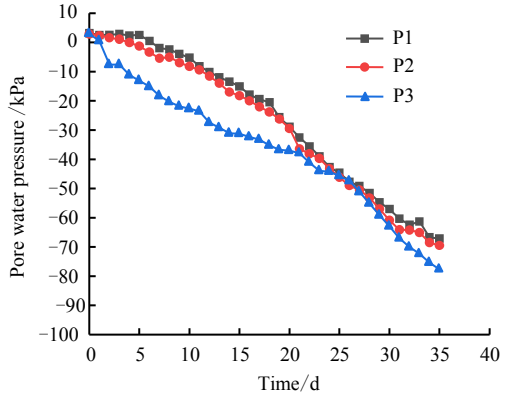

(a) Conventional vacuum preloading（Test A）

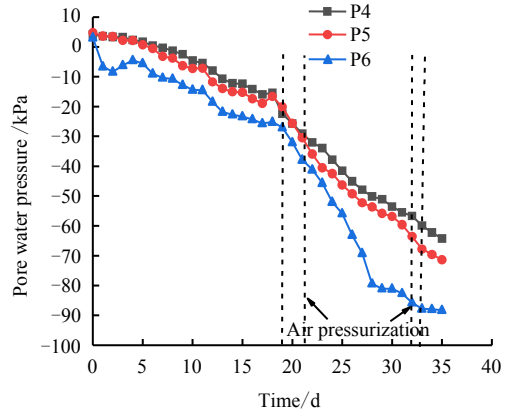

(b) Air-booster vacuum preloading（Test B）

Fig.4 Variations of pore water pressure with respect to time

3.3 Vane shear strength

Using the mini-vane shearing instrument, the shear strength was measured for the soil of both buckets when the vacuum preloading ended. Two test locations, i.e. 10 cm and 20 cm radially away from the PVD, were chosen. And at each location, the test was carried out at 0 cm, 15 cm, and 30 cm below the soil surface, respectively. Test results on the shear strength are shown in Fig.5. It is obvious that shear strength at the test point from Test B is larger than the value at the corresponding location from Test A. Specifically, for the soil 10 cm radially away from the PVD, the average shear strength of Test B is 1.14 times larger than that of Test A; and for the soil 20 cm radially away from the PVD, the former is 1.13 times higher than the latter. The comparison demonstrates that the air-booster vacuum preloading technology can help improving the soil strength.

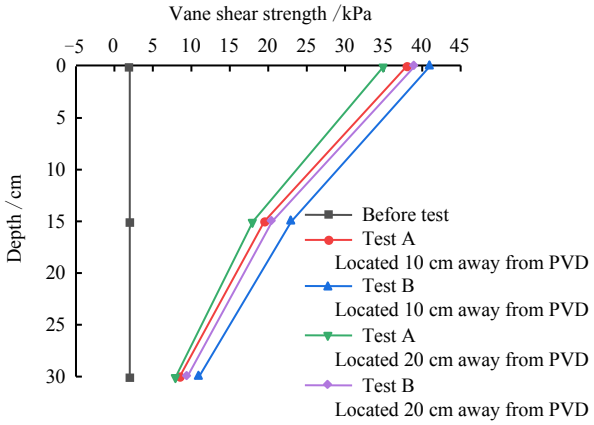

Fig.5 Vane shear strength after reinforcement

4 Real-time pore water pressure response

In Section 3, three common engineering indexes including settlement, PWP dissipation, and shear strength are investigated to show the favorable effects of air pressurization on vacuum consolidation of slurry. However, current studies on the real-time PWP response during the air boosting period (e.g., 10 mins per day for present tests) are limited in the literature. To this end, the real-time PWP response during the first air boosting period are presented in Figs.6(a), (b),and (c), respectively, for the 19th, 20th and 21st day of Test B. The three figures show similar variations in PWP response with respect to time, i.e. the PWP increases to a stable value within 60 s after the start of boosting; for the time after, the PWP fluctuates slightly around the stable value; and then the PWP decreases rapidly when the boosting stops. Take Fig. 6(a) as an example, the largest increase in PWP is observed for transducer P4 (the closest one to the booster tube) when compared to the other transducers, i.e., the PWP of P4 increases 15.3 kPa (from -14.9 kPa to 0.4 kPa) shortly after the activation of the booster pump. For transducers P5 and P6, the increases in PWP are 12 kPa and 2.5 kPa, respectively. Since the PWP difference between P4 and P6 increases from 10 kPa before the boosting to 23 kPa after the boosting, the hydraulic gradient measured radially between the booster tube and the PVD is improved accordingly during the air boosting period. As a result, the seepage consolidation of the slurry between the booster tube and the PVD is enhanced. At the moment the boosting stops, the PWPs at P4, P5 and P6 drops rapidly to -22.4 kPa, -20 kPa and -27 kPa, respectively, which are 7.5 kPa, 3.8 kPa and 2.1 kPa lower than the corresponding values recorded before the boosting.

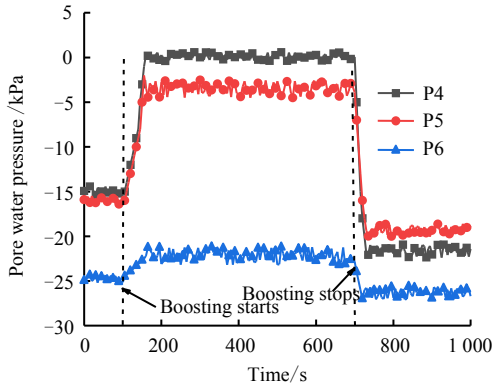

(a) On the 19th day（boost duration10 min）

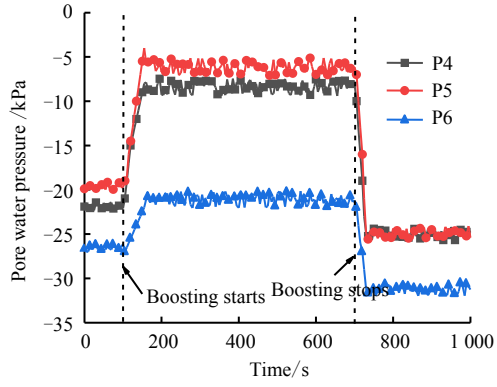

(b) On the 20th day（boost duration10 min）

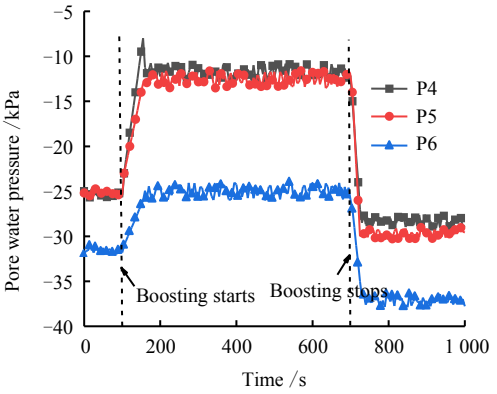

(c) On the 21st day（boost duration10 min）

Fig.6 Real-time variations of pore water pressure during the first air pressurization in barrel B

The drop in PWP indicates that the soil between the booster tube and the PVD is largely in an undrained condition. As a result, most of the air pressure is carried by the pore water, and then the PWP drops rapidly once the air pressure stops, since the compressibility of the pore water is very low. However, it is noted that the PWP will drop to a lower value than that right before the boosting, which means part of the excess PWP is transferred into the effective stress of the soil skeleton within the 10 mins duration of the boosting. Consequently, the unloading expansion of the soil skeleton due to termination of boosting generates negative PWP in soil, i.e., -7.5 kPa, -3.8 kPa, and -2.1 kPa at transducers P4, P5, and P6, respectively. The change in effective stress of the soil skeleton indicates that seepage consolidation happens during the boosting. Based on the one-dimensional consolidation theory established for the soil between the booster tube and the PVD, the soil permeability that governs the seepage during the boosting can be estimated, and it is in the order of 10^{-6} m/s. Similarly, according to the radial drainage consolidation theory, the soil permeability before the first boosting is estimated as in the order of 10^{-8} m/s using the recorded PWP dissipation values. Details of both estimations are given in Appendix A. That is to say, the soil permeability has been improved by two orders of magnitude by the air pressurization. The comparison indicates that micro cracks may generate within the soil during the boosting, which substantially increases the overall soil permeability. Those cracks continue to promote the PWP dissipation even though the boosting stops, as can be seen from Fig.4.

5 Discussion

The real-time PWP response in Section 4 demonstrates that the air pressurization in soil leads to two folds of consequences. The first consequence is the increased hydraulic gradient between the booster tube and the PVD, which increases the seepage velocity of pore water, and thus increases the drainage and thus improves the effect of vacuum consolidation. However, the increased gradient disappears once the air boosting stops. The second consequence is the possible micro cracks generated within the soil due to the pressurized air, which effectively increases soil permeability. Moreover, these cracks remain open after the boosting stops and keep providing drainage paths for pore water , and thus improve PWP dissipation and seepage consolidation.

First, let us assume that the increased hydraulic gradient is the only reason for the positive effects on vacuum consolidation by the air boosting. A finite element model was constructed to simulate Test B using ABAQUS. The PVD with a rectangular section was simulated as a cylinder with an equivalent diameter 0.06 m. Linear elastic response was assumed for the soil in the numerical model, i.e. no cracks shall be generated. The same elastic modulus (0.04 MPa) and Poisson's ratio (0.3) were assigned to the soil and the PVD. The permeabilities of the soil and the PVD were taken as 1×10^{-8} m/s and 1×10^{-5} m/s, respectively. No-displacement and no-flux boundary conditions were set to the bottom of the model. The boundary conditions for the side of the model were taken as zero flux and traction free (to consider the radially inward displacement of soil during the vacuum consolidation). The boundary conditions on top of the model were taken the same as those for the side boundaries to model the effects of the airtight membrane. The excess pore water pressure of the PVD was set to -80 kPa to simulated the vacuum pressure. A positive pressure of 20 kPa was set to the soil elements occupying the volume of the booster tube (i.e. the booster tube was not explicitly modeled) in a Heaviside-function manner to generate the increased hydraulic gradient between the booster tube and the PVD. The settlement monitor point was at the center of the top surface, and the monitor point for both the PWP and the seepage velocity was at

the midpoint of an imaginary line that connecting the top of the booster tube and the middle of the PVD.

The numerical results on settlement and PWP dissipation are presented in Figs.7 and 8 for the comparison between the cases with and without the air boosting. It is clear that the response for the two cases are the same for the period before the boosting. For the period of boosting, the PWP increases abruptly along with a slight rebound in settlement. The comparisons indicate that the increased hydraulic gradient plays adverse effects on the settlement and the PWP dissipation. However, the seepage velocity increases during the boosting, as shown in Fig.9. However, from Fig.9 it is seen that the increased velocity lasts only for the short period of the boosting (i.e. 10 mins per day). Actually, the contribution of the increased seepage velocity within the short period of the boosting (10 mins/day in 3 consecutive days in present study) is insignificant as compared to the accumulated drainage volume within the entire treatment period (35 days in present study). This observation excludes the increased hydraulic gradient as the main reason for the positive effects by air boosting, which indicates that the micro cracks contribute to the improved settlement, shear strength and PWP dissipation observed in Test B. The micro cracks generated by the pressurized air would remain open and thus improve seepage for both the time periods during and after the boosting-a strong contrast to the increased hydraulic gradient that is only effective during the boosting.

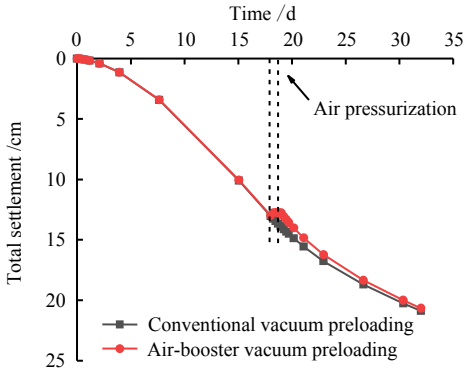

Fig.7 Time variations of surface settlement from numerical simulation

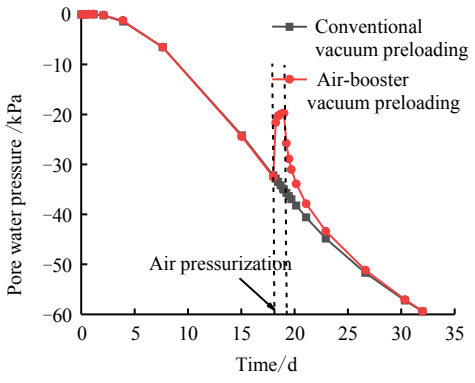

Fig.8 Time variations of pore water pressure from numerical simulation

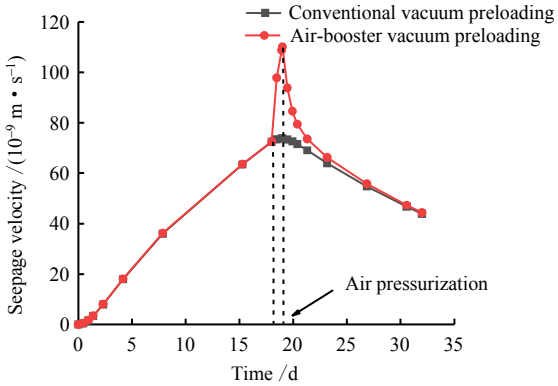

Fig.9 Time variations of seepage velocity from numerical simulation

The increased hydraulic gradient is similar to lateral loading on the soil between the boosting tube and the PVD. It is clear that the effects of vacuum consolidation can be effectively improved only when the duration of the lateral loading is comparable to that of the vacuum treatment. However, in practice implementation of the air-booster vacuum preloading technology, the air pressurization is applied typically at the late stage during the vacuum treatment period, and the boost bump typically works in an intermittent manner, e.g. 2-8 hours per day within 10-15 consecutive days (out of the total treatment period 90 d). Also, it is concluded from practical experiences that no obvious effect would be generated if the boosting duration is elongated, let alone the great risk of the airtight membrane being blown up by the boosted air and thus the possible failure of the whole sealing system. Ideally speaking, the air boosting is expected to initiate only micro cracks extending laterally from the booster tube to the PVD, but without the large ones that propagate to the ground surface. Obviously, this idealized situation can only happen if proper settings are taken for the boosting pressure, the duration of the boosting and the time when to activate the boosting, which certainly requires more elaborations both in laboratory, field test and numerical modeling studies.

6 Conclusions

The conventional and air-booster vacuum preloading technologies were implemented into two parallel model tests on dredged slurry in this paper. Typicaly engineering indice including settlement, accumulated pore water pressure (PWP) dissipation, and undrained shear strength were measured and compared between the two technologies. Specially, the real-time PWP response during the air boosting were recorded and analyzed. The following conclusions can be drawn.

(1) The air-booster vacuum preloading technology is superior to the conventional vacuum preloading technology, as the settlement, the accumulated PWP dissipation and the shear strength of the former are 20.5%, 5.7% and 1.13%, respectively, higher than those of the latter.

(2) The real-time PWP response demonstrates that the air pressurization in soil is leads to two folds of consequences. One is the increased hydraulic gradient between the booster tube and

the PVD, which enhances the seepage velocity and thus the drainage consolidation correspondingly. The second consequence is the possible micro cracks generated within the soil mass by the pressurized air. The cracks that provide high permeable and shorter drainage paths can effectively improve the drainage consolidation of slurry for both during and after the boosting period.

(3) After comparing to the computational results from ABAQUS, it is found that the increased hydraulic gradient contributes little to the consolidation effects by vacuum preloading, which makes the micro cracks as the only reason for the improved settlement, shear strength and PWP dissipation as observed in the air-booster vacuum preloading technology. The micro cracks generated by the pressurized air would remain open and thus improve seepage for both during and after the boosting period.

References

[1] WANG Jun, CAI Yuan-qiang, FU Hong-tao, et al. Indoor and field experiment on vacuum preloading with new anti-clogging measures[J]. Chinese Journal of Rock Mechanics and Engineering, 2014, 33(6): 1257-1268.

[2] JIANG Yan-bin, HE Ning, XU Bin-hua, et al. Model test of vacuum preloading negative pressure distribution[J]. Chinese Journal of Geotechnical Engineering, 2017, 39(10): 1874-1883.

[3] CAO Jie, ZHENG Jian-guo, LIU Zhi, et al. Engineering application of vacuum preloading method in soft soil foundation treatment[J]. Chinese Journal of Geotechnical Engineering, 2017, 39(Suppl. 2): 124-127.

[4] HUANG Chao-yuan, WANG Zheng-zhong, FANG Yong-lai. Analytical solution of vacuum preloading foundation consolidation considering non-linearity of gas leakage and well resistance[J]. Rock and Soil Mechanics, 2017, 38(9): 2574-2582.

[5] LIU Zhi-zhong, DING Jian-wen, WANG Gang, et al. Vacuum preloading settlement calculation method considering vacuum attenuation[J]. Journal of Southeast University (Natural Science Edition), 2016, 46(1): 191-195.

[6] YAN S W, CHU J. Soil improvement for a storage yard using the combined vacuum and fill[J]. Canadian Geotechnical Journal, 2005, 42(4): 1094-1104.

[7] CHU J, YAN S W, YANG H. Soil improvement by the vacuum preloading method for an oil storage station[J]. Geotechnique, 2000, 50(6): 625-632.

[8] JIANG Yan-bin, HE Ning, ZHOU Yan-zhang, et al. Research on the concept and measurement technology of vacuum preloading groundwater level[J]. Chinese Journal of Geotechnical Engineering, 2016, 38(10): 1917-1922.

[9] SUN Li-qiang, YAN Shu-wang, LI Wei, et al. Study of super-soft soil vacuum preloading model test[J]. Rock and Soil Mechanics, 2011, 32(4): 984-990.

[10] LIU S Y, ZHANG D W, DU G Y, et al. A new combined vacuum preloading with pneumatic fracturing method for soft ground improvement[J]. Procedia Engineering, 2016, 143: 465-461.

[11] CHEN Geng, HONG Xiu-min, WANG Bo, et al. Laboratory test of plastic drain filter clogging under vacuum preloading[J]. China Harbour Engineering, 2016, 36(1): 23-27.

[12] SHI L, WANG Q Q, XU S L, et al. Numerical study on clogging of prefabricated vertical drain in slurry under vacuum loading[J]. Granular Matter, 2018, 10:20-74.

[13] WANG J, NI J, CAI Y Q, et al. Combination of vacuum preloading and lime treatment for improvement of dredged fill[J]. Engineering Geology, 2017, 227: 149-158.

[14] WANG Jun, ZHANG Le, LIU Fei-yu, et al. Experimental study of vacuum preloading combined reinforcement with electro-osmosis in soft clay ground[J]. Chinese Journal of Rock Mechanics and Engineering, 2014, 33(Suppl.2): 4181-4192.

[15] CAI Y Q, XIE Z W, WANG J, et al. New approach of vacuum preloading with booster prefabricated vertical drains (PVDs) to improve deep marine clay strata[J]. Canadian Geotechnical Journal, 2018, 10: 1359-1371.

[16] SHEN Yu-peng, FENG Rui-ling, YU Jiang, et al. Reinforcement of vacuum preloading with air pressure boosted for soft ground treatment[J]. Journal of Jilin University (Earth Science Edition), 2012, 42(3): 792-797.

[17] ZHU Ping, SUN Li-qiang, YAN Shu-wang, et al. Model test of vacuum preloading with controlled ventilation and its mechanism analysis[J]. Chinese Journal of Rock Mechanics and Engineering, 2011, 30(Suppl.1): 3141-3148.

[18] YAN Shu-wang, ZHANG Li-li, SUN Li-qiang, et al. Experimental research on the method of importing air flow to accelerate drainage in vacuum pre-pressure[J]. Highway Transportation Technology (Applied Technology Edition), 2011, 7(1): 30-33+46.

[19] ZHANG Ding-wen, LIU Song-yu, GU Chen-ying, et al. Model tests on pneumatic fracturing in soils[J]. Chinese Journal of Geotechnical Engineering, 2009, 31(12): 1925-1929.

[20] ZENG Fang-jin, WEI Hui-xing, WANG Jun, et al. Laboratory model test of treating soft soil ground using deep air-boosted vacuum preloading[J]. Industrial Construction, 2014, 44(7): 90-94.

[21] SHEN Yu-peng, YU Jiang, LIU Hui, et al. Experimental study on air-boosted vacuum preloading of soft station

foundation[J]. Journal of the China Railway Society, 2011, 33(5): 97-103.

[22] LIN Yan, LI Biao, ZHUGE Ai-jun. Application of air-boosted vacuum preloading on soft soil foundation treatment in Lianyungang[J]. China Harbour Engineering, 2016, 36(11): 46-51.

Appendix A

A.1 Estimation on bulk modulus of pore water

Based on Biot's theory, the excess pore water pressure is related to the volumetric strains of the soil skeleton θ and the pore water ζ by

$$p=-\frac{K_{\mathrm{f}}}{n}(\alpha\theta+\zeta) \tag{A1}$$

where K_{f} is the bulk modulus of pore water; n is the porosity; $\alpha=1-K/K_{\mathrm{s}}$, K is the bulk modulus of soil skeleton, K_{s} is the bulk modulus of soil grain. $\alpha\approx1$ because $K\ll K_{\mathrm{s}}$.

The variations of accumulated drainage mass with respect to time are presented in Fig.A.1 for both Tests A and B. The drainage volume (=drainage mass divided by density of water 1.0 g/cm^3) during 5 days (i.e. the 14th−18th day) before the first boosting is extracted from the figure and then put in Table A1 for Test B. The incremental drainage volume between two consecutive days can be obtained by subtracting the drainage volume on Day n-1 from that on Day n, where n=15, …, 18. Then, the volumetric strain of pore water on Day n is calculated as the incremental drainage volume divided by volume V_{s} of slurry on Day n. V_{s} equals to $\pi D^2(H_0-s)/4$, where D is the diameter of the bucket; H_0=0.55 m is the initial height of the slurry; s is the measured settlement on Day n (see Fig. 3).

The volumetric strains for the two periods (i.e. the 16th −18th days and the 15th−17th days) are averaged, respectively. And subtracting between them gives the incremental volumetric strain of the pore water $\Delta\zeta=-5.850\ 7\times10^{-4}$ for the period shortly before the first boosting.

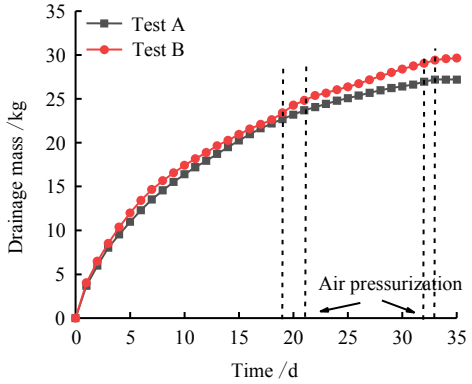

Fig.A1 Variations of cumulative drainage mass over time

Table A1 Volumetric strains for pore water

Time /d	Drainage volume /m^3	Incremental drainage volume /m^3	Volume of soil in Test B/m^3	Volumetric strain of pore water
14	$2.026\ 2\times10^{-2}$	–	–	–
15	$2.093\ 7\times10^{-2}$	6.75×10^{-4}	$8.698\ 0\times10^{-2}$	$7.760\ 4\times10^{-3}$
16	$2.156\ 2\times10^{-2}$	6.25×10^{-4}	$8.639\ 3\times10^{-2}$	$7.234\ 3\times10^{-3}$
17	$2.209\ 5\times10^{-2}$	5.33×10^{-4}	$8.501\ 9\times10^{-2}$	$6.269\ 2\times10^{-3}$
18	$2.260\ 2\times10^{-2}$	5.07×10^{-4}	$8.443\ 0\times10^{-2}$	$6.005\ 0\times10^{-3}$

By following the same procedure depicted for Table A1, the incremental volumetric strain of the soil skeleton for the same period before the first boosting can be determined as $\Delta\varepsilon_z=1.297\ 5\times10^{-4}$, according to the measured settlement development in Fig.3.

The spherical incremental stress is applied to the soil skeleton through vacuum pressure. With the assumption of homogeneity of the dredged slurry, the volumetric strain of the soil skeleton can be estimated as

$$\Delta\theta=3\Delta\varepsilon_z=3.892\ 6\times10^{-4} \tag{A2}$$

By following the same procedure depicted for Table A1, the incremental pore water pressure for the same period before the first boosting can be determined as $\Delta p=1.296$ kPa.

According to the measured pore water pressure variation in Fig.4. Substituting $\Delta\zeta$, $\Delta\theta$ and Δp into Eq. (A1), the bulk modulus of pore water K_{f} divided by the porosity n can be obtained as $\frac{K_{\mathrm{f}}}{n}=6.4751\times10^3$ kPa.

A.2 Estimation of soil permeability for boosting period

From Section 4, it is known that the unloading expansion of the soil skeleton triggered by the termination of the boosting generates negative pore water pressure in soil, i.e., -7.5 kPa, -3.8 kPa and -2.1 kPa at transducers P4, P5 and P6, respectively. After substituting a representative value of -3.8 kPa into Eq. (A1), the volumetric strain of soil skeleton due to unloading expansion can be calculated as (the soil is assumed as undrained at the moment of unloading, i.e. ζ=0)

$$\theta=-\frac{np}{K_{\mathrm{f}}}=\frac{3.8}{6\ 475.1}=5.868\ 6\times10^{-4} \tag{A3}$$

From the compression-rebound curve of the tested slurry (see Fig.A2, the void ratios at different pressure levels are explicitly given in Table A2), the unloading bulk modulus of the soil skeleton can be estimated as $K_{\mathrm{u}}=3.372\ 3\times10^3$ kPa. Accordingly, the effective stress for unloaded is given as

$$\Delta\sigma'=\theta K_{\mathrm{u}}=1.979\ \mathrm{kPa} \tag{A4}$$

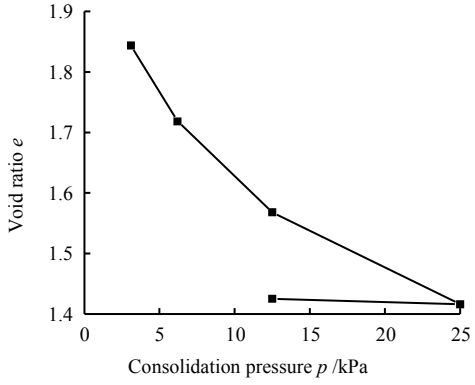

Fig.A2 Compression-rebound curve of test soil

Table A2 Porosity variations under different consolidation pressures

Consolidation pressure p /kPa	3.1	6.2	12.5	25.0	12.5
Void ratio e	1.843	1.718	1.568	1.416	1.425

In other words, during the process (10 mins) of air boosting (the boosting pressure for the soil is 12 kPa, as given by the pore water pressure transducer P5), the soil has undergone drainage consolidation and gained an effective stress of 1.797 kPa. Since the booster tube is pervious, the soil between the tube and the PVD can be assumed as one-dimensional consolidation with double drainage boundaries, i.e. one is at the pervious tube surface, and the other is at the PVD filter membrane. Then, Terzaghi's one-dimensional consolidation theory can be readily applied

$$U=1-\frac{8}{\pi^2}\sum_{m=1}^{\infty}\frac{1}{m_2}\exp\left(-\frac{m^2\pi^2T_{\rm v}}{4}\right)(m=1,3,5,\ldots) \tag{A5}$$

where U is the degree of consolidation; $T_{\rm v}=C_{\rm v}t/H^2$ is the time factor of consolidation; $C_{\rm v}$ is the coefficient of consolidation; t is time; H is the drainage distance. According the incremental effective stress $\Delta\sigma'$, the consolidation degree is determined as U=1.979/12= 16.49%.

Substituting H=0.1 m (obtained from Fig. 2) and t=10 mins into Eq. (A5), $C_{\rm v}$ =3.56×10^{-7} m^2/s can be back calculated. $C_{\rm v}$ is related to the soil permeability k and the volumetric compressibility coefficient $m_{\rm v}$ of the soil as

$$C_{\rm v}=k/(m_{\rm v}\gamma_{\rm w}) \tag{A6}$$

where $\gamma_{\rm w}$ is the unit weight of water. From Fig.A2, $m_{\rm v}$ = 4.735 8×10^{-3} kPa^{-1} can be obtained for the pressure in range of 12.5-25.0 kPa. Then, from Eq. (A6) the soil permeability k = 1.685 9×10^{-8} m/s can be determined.

A.3 Estimation of soil permeability before air boosting

The drainage consolidation of the slurry can be described using the radial drainage consolidation theory by Hansbo for the vacuum preloading before the boosting. The diameter ratio $n_{\rm w}$ is

$$n_{\rm w}=\frac{d_{\rm e}}{d_{\rm w}}=\frac{0.5}{0.066}=7.55 \tag{A7}$$

where $d_{\rm e}$ and $d_{\rm w}$ are equivalent diameters of the influence area and the PVD, respectively. With $n_{\rm w}$, the dimensionless factor $F_{\rm n}$ is determined by

$$F_{\rm n}=\frac{n_{\rm w}^2}{n_{\rm w}^2-1}\ln n_{\rm w}-\frac{3n_{\rm w}^2-1}{4n_{\rm w}^2}=1.312 \tag{A8}$$

The average degree of consolidation in radial direction is given by

$$\overline{u}_{\rm r}=1-{\rm e}^{-\frac{8C_{\rm h}}{F_{\rm n}d_{\rm e}^2}t} \tag{A9}$$

and

$$C_{\rm h}=\frac{k}{m_{\rm v}\gamma_{\rm w}}=21.12k \tag{A10}$$

After substituting $C_{\rm h}$、$F_{\rm n}$ and $d_{\rm e}$ into Eq. (A9), the degree of consolidation can be expressed as

$$\overline{u}_{\rm r}=1-{\rm e}^{-515.12kt} \tag{A11}$$

With the time t =18×24×3 600=1.555 2×10^6 s taken right before the first boosting, $\overline{u}_{\rm r}$ is expressed as

$$\overline{u}_{\rm r}=1-{\rm e}^{-515.12kt}=1-{\rm e}^{-8.01\times10^8k} \tag{A12}$$

Since the accumulate pore water pressure dissipation right before the first boosting is Δu =25 kPa, the degree of consolidation expressed in pore water pressure dissipation is calculated as

$$\overline{u}_{\rm r}=\frac{\Delta u}{p}\times100\%=\frac{25}{80}\times100\%=31.3\% \tag{A13}$$

Substituting Eq. (A13) nto Eq. (A12), the soil permeability averaged over the period before the first boosting is obtained as k = 4.686 9×10^{-10} m/s.